Aalborg Universitet

Experimental Characterization of Delay and Age of Information in DSRC V2V

Jiménez-Soria, David; Soret, Beatriz; Aguayo-Torres, M. Carmen

Published in:
2022 IEEE 96th Vehicular Technology Conference (VTC2022-Fall)

DOI (link to publication from Publisher):
10.1109/VTC2022-Fall57202.2022.10012741

Publication date:
2022

Document Version
Accepted author manuscript, peer reviewed version

Link to publication from Aalborg University

Citation for published version (APA):
Jiménez-Soria, D., Soret, B., & Aguayo-Torres, M. C. (2022). Experimental Characterization of Delay and Age of Information in DSRC V2V. In *2022 IEEE 96th Vehicular Technology Conference (VTC2022-Fall)* (pp. 1-7). Article 10012741 IEEE (Institute of Electrical and Electronics Engineers). https://doi.org/10.1109/VTC2022-Fall57202.2022.10012741

General rights
Copyright and moral rights for the publications made accessible in the public portal are retained by the authors and/or other copyright owners and it is a condition of accessing publications that users recognise and abide by the legal requirements associated with these rights.

- Users may download and print one copy of any publication from the public portal for the purpose of private study or research.
- You may not further distribute the material or use it for any profit-making activity or commercial gain
- You may freely distribute the URL identifying the publication in the public portal -

Take down policy
If you believe that this document breaches copyright please contact us at vbn@aub.aau.dk providing details, and we will remove access to the work immediately and investigate your claim.

Downloaded from vbn.aau.dk on: November 10, 2025

Experimental Characterization of Delay and Age of Information in DSRC V2V

David Jiménez-Soria, Beatriz Soret, M. Carmen Aguayo-Torres

Abstract—**In this paper, we demonstrate the real-time performance of Dedicated Short Range Communication (DSRC) through the design and development of a full-stack testbed based on open-source software that includes the IEEE 802.11p and the IEEE 1609 protocol suite. Vehicles broadcast periodic Basic Safety Messages (BSM). Reference mobility and data traffic models from 3GPP are used for scenario generation using ns-3. We show how to meet the timing requirements of the 802.11p lower layers using low-cost, commercial off-the-shelf components, based on open-source GNU Radio and tested with Ettus USRP B210 Software Defined Radio (SDR), 6 GHz Tx/Rx RF frontends and GPS Disciplined Oscillator (GPSDO). The testbed is used to characterize the different contributors to the total delay budget and the Age of Information (AoI), a key metric for vehicle-to-vehicle (V2V). We observe that the AoI is impacted not only by the communication parameters but also by the mobility and traffic conditions. Our results show that more frequent BSM transmission reduces the average peak age but with a higher value relative to the inter-BSM period due to the collisions and packet losses.**

I. Introduction

The Vehicle-to-Vehicle (V2V) communication in Intelligent Transport Systems (ITS) relies on vehicles broadcasting safety-critical information such as vehicle position, speed and heading for tracking purposes. The final goal is to increase road safety through applications like the electronic emergency brake light or slow/stopped vehicle alerts. There are two prominent V2V technologies: (1) the WiFi-based Dedicated Short-Range Communication (DSRC) [1], developed by IEEE and enabling vehicles to communicate with each other without involving cellular or other infrastructure; (2) and the 3rd Generation Partnership Project (3GPP) Cellular Vehicle-to-Everything (C-V2X), based on the 4G Long Term Evolution (LTE). Both solutions broadcast safety status messages – called Basic Safety Message (BSM) in DSRC – although the lower layers present significant differences.

The Age of Information (AoI) [2] has attracted significant attention in the last decade [3] for tracking or monitoring applications that transmit update messages. The AoI is a process that measures the time elapsed since the generation of the last received status update. Following the original paper of Kaul [2], there has been a huge amount of works analyzing and optimizing the AoI and its byproducts, such as the Peak Age of Information (PAoI), in different scenarios [4]. Much less effort has been devoted to the comparison of the analyses and simulations with experimental results. The implementation of the entire application and communication system has not been either sufficiently studied, although the generation process and the upper layers are known to have a great impact in the AoI. One exception is [5], where live experiments over the Internet allow the analysis of the impact of the transport layer protocols.

The BSM transmission in DSRC (and its C-V2X counterpart) has been widely studied in the literature, mostly focusing on the Medium Access Control (MAC) performance. In [6], the backoff counter in the IEEE 802.11p MAC protocol is selected based on the historical data from the other vehicles. The transmission of BSM is an example of timing-sensitive application where the broadcast should be optimized not for packet losses but for freshness and value of the information [7]. In this regard, recent papers have looked at different AoI optimizations and how it relates to the on-road safety (see, e.g., [8], [9]), although none of them has verified the analysis or simulations with real-tests. The set of works presenting DSRC implementations and real-time results is much smaller, and mainly centered around the packet losses and the field testing. We find research papers that present the integration of available commercial solutions, like [10], where UBlox modules are road-tested under different conditions. Specifically, the impact of the propagation conditions in the packet losses is investigated. Others have developed the lower layer protocols: [11] proposes an open source implementation and compares it to commercial solutions, whereas [12] presents application level results of a testbed that implements the regular TCP/UDP-IP stack in the upper layers rather than the IEEE 1609 family. An important aspect of DSRC results is the selection of realistic scenarios for the mobility and the data traffic. In this regard, 3GPP provides a complete reference scenario in [13]. To the best of our knowledge, the AoI has not been evaluated in real-time implementations.

The contribution of this paper is two-fold: (1) We present the design and development of a full-stack DSRC vehicular networking testbed using the fully open-source Software Defined Radio (SDR) testbed V2Verifier [14], the mobility scenarios from 3GPP [13] using ns-3 [15] and the Abstract Syntax Notation One (ASN.1) definition of the BSMs. We demonstrate that a real-time implementation is feasible using low-cost hardware, based on GNURadio and tested with Ettus USRP B210 SDR. (2) We use the testbed to characterize the total delay budget, and to measure the AoI, the PAoI and the Packet Delivery Ratio (PDR). We quantify the impact of the communication parameters and the traffic conditions in the AoI, and observe the unavoidable tradeoff between AoI and reliability.

David Jiménez, Beatriz Soret and M. Carmen Aguayo-Torres (email: djs@ic.uma.es, bsoret@ic.uma.es, aguayo@ic.uma.es) are with the Telecommunication Research Institute (TELMA), Universidad de Málaga, Spain. B. Soret is also with the Connectivity Section in Aalborg University, Denmark.

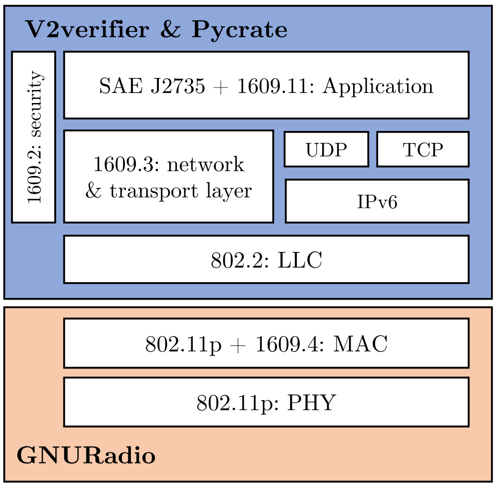

Fig. 1. DSRC protocol stack

II. Preliminaries

Fig. 1 shows the core protocol stack, where IEEE 802.11p covers the PHYsical layer (PHY) and lower MAC, whereas the upper layers are defined in the IEEE 1609 family of standards. This core part of DSRC is called IEEE Wireless Access in Vehicular Environments (WAVE), although the terms DSRC and WAVE are sometimes used arbitrarily. DSRC utilizes the band $5.85 - 5.925$ GHz.

A. IEEE 1609 protocol suite and Society of Automotive Engineers (SAE) J2735

The IEEE 1609 suite comprises the security services in 1609.2, the network services in 1609.3 to set various transmission parameters, and the channel switching in 1609.4. BSMs are standardized in the SAE J2735 standard [16], which defines not only the ASN.1 format but also additional requirements on how to use them. The messages have two parts. The first part is mandatory and contains core information about the vehicle (e.g., its size) and its status (e.g., speed, position, and accelerations). The second part is optional and adds a variable number of event-related data, such as notifications about the activation of safety-related subsystems within the vehicle (e.g., the activation of the ABS system) or the path history.

B. IEEE 802.11p

IEEE 802.11p is a part of the IEEE 802.11 standard and is specially designed to support the high mobility outdoor environment of vehicular communications. The spectrum is divided into up to seven 10 MHz channels, with a guard band of 5 MHz. The Service Channel (SSH) and the Control Channel (CCH) can be interspersed using different channel access configurations (continuous, alternating, immediate or extended). All vehicles are synchronized to listen to the CCH when corresponding for safety-related and system control exchange. The IEEE 802.11p PHY uses Orthogonal Frequency Division Multiplexing (OFDM) modulation scheme to multiplex data, with a Fast Fourier Transform (FFT) size of 64 and 52 subcarriers (48 data subcarriers and four pilot subcarriers). The BSMs are broadcasted in the CCH. As soon as a new message is generated, the vehicle starts the channel access procedure, eventually broadcasting the message using Carrier Sense Multiple Access with Collision Avoidance (CSMA/CA) as specified in the IEEE 802.11p MAC protocol. The vehicle starts by listening to the channel. If the channel is idle for an Arbitration Interframe Space (AIFS) or a DCF Interframe Space (DIFS) time, then the vehicle can start transmitting directly. If the channel is busy or becomes occupied during the AIFS/DIFS, then the vehicle must perform a backoff, that is, the node has to defer its access according to a randomized time period. When the backoff counter hits 0, the vehicle transmits. There is no Acknowledgement (ACK) or retransmission mechanism. The message is dropped if it is not sent by the end of the control channel, as a new beacon will be generated in the next channel cycle.

C. Time synchronization

Maintaining a unique temporal reference system is very important in ad-hoc-based communications where there is no common infrastructure but a highly dynamic and decentralized network. In DSRC, channel access is synchronized using Coordinated Universal Time (UTC) for a global time reference which is provided by a global satellite navigation system, e.g., Global Positioning System (GPS) [17]. The IEEE 802.11p specification [18] reflects the importance of using synchronization techniques by means of timing advertisement frames, which allows IEEE 802.11p stations to synchronize themselves with a common time reference or may be used to assist in time synchronisation if GPS signals become unavailable.

In simulation, every node is assumed to be time synchronized with sufficient accuracy. In a real environment, each device has a GPS module that provides the time synchronization signal. Unlike simulations, the synchronization of transmitter and receiver is critical in a real-time test where the goal is to obtain reliable timing measurements. For the time requirements of DSRC and the selected software and hardware components in the testbed, the GPSDO has been proven to be sufficiently accurate, as described later.

D. Delay and AoI in V2V

We consider a set of $\mathcal{V}$ vehicles exchanging BSMs of size D bits. Frame capture is implemented as follows. If the new incoming frame arrives while the receiver is receiving the preamble of another frame and the Signal to Interference Ratio (SIR) of the new incoming frame is above a fixed margin, then the current frame is dropped and the receiver locks onto the new incoming frame. All vehicles use the same modulation (BPSK) and coding rate (1/2). The timing metrics, delay and AoI are defined for a pair of source-destination vehicles. We define a probe vehicle p and assume that p can be reached by $\mathcal{W} \subseteq \mathcal{V}$ neighbouring vehicles. We denote $g = [g_1, ..., g_{i-1}, g_i, g_{i+1} ..., g_n]$, $t = [t_1, ..., t_{i-1}, t_i, t_{i+1} ..., t_n]$ and $r = [r_1, ..., r_{i-1}, r_i, r_{i+1}, ..., r_n]$ the vectors of generation, transmission and reception times of the BSM received at p,

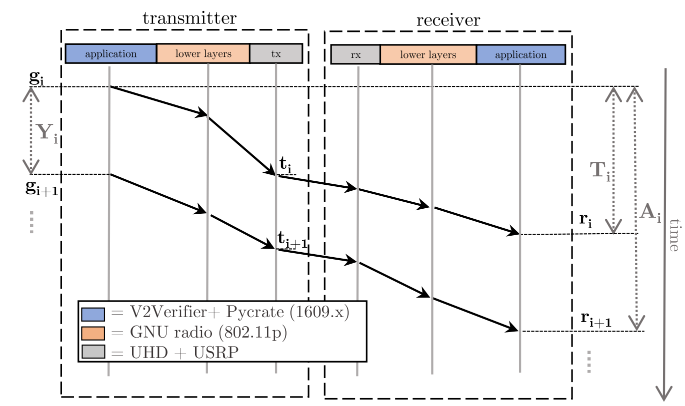

Fig. 2. Schematic of the timing in the real-time testbed, showing the transmission of BSMs i and $i+1$. g_i, t_i and r_i are the generation, transmission and reception times of packet i, respectively. The difference $T_i = r_i - g_i$ represents the system time.

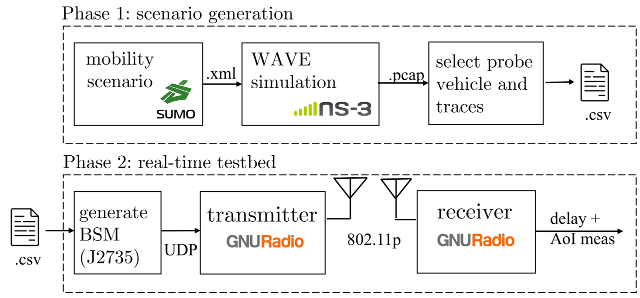

Fig. 3. Testbed block diagram.

respectively. Moreover, $Y_i = g_{i+1} - g_i$ is the inter-arrival time and $T_i = r_i - g_i$ is the system time of the ith BSM, respectively.

The packet delay is defined as the time difference between the reception time and the transmission time, i.e., $r_i - t_i$. The average end-to-end delay, not depending on the generation process but only on the communications phase, is then measured as

$$\bar{\delta}^{meas} = \frac{\sum_{i=1}^{n}(r_i - t_i)}{n} \tag{1}$$

We define the AoI as the time that has elapsed since the newest BSM available at the probe vehicle p at time t was generated at the source vehicle s. The AoI is the process $\Delta(t) = t - \mathrm{U}(t)$, where $\mathrm{U}(t)$ is the generation time (i.e. time stamp) of the newest BSM that the probe p has received from source s by time t. This definition leads to a sawtooth pattern in the temporal evolution of the metric [2] that we will discuss in the results of Section IV.

In the real-time testbed, our interest is in the evaluation of Δ from the experiments. It is straightforward to use geometric arguments to calculate the trapezoid areas that contribute to the AoI [19], which are given in terms of the reception times r_i and the generation times g_i,

$$Q_i = \frac{1}{2}\left[((g_{i+1} - g_i) + (r_i - g_i))^2 - (r_i - g_i)^2\right] \tag{2}$$

The average AoI is then estimated as follows

$$\bar{\Delta}^{meas} = \frac{\sum_{i=2}^{n} Q_i}{r_n - g_2} \tag{3}$$

We can also define the peak age of the ith BSM as the value of AoI achieved immediately before receiving the ith update, i.e., $A_i = Y_i + T_i$.

From the experimental data, the average PAoI is evaluated as

$$\bar{A}^{meas} = \frac{\sum_{i=1}^{n-1}(r_{i+1} - t_i)}{n-2} \tag{4}$$

Fig. 2 shows an schematic of the transmission of BSM and the different parameters defined, relating also to the protocol stack components and contribution to the total delay and age.

III. Testbed Implementation

Fig. 3 depicts the block structure of the full-stack testbed, showing the different software and hardware components, as well as the interconnection interfaces. The execution is divided into the next two phases:

- Phase 1: In this phase, the mobility scenario is first defined and simulated using Simulation of Urban MObility (SUMO). The parameters are selected from the 3GPP simulation environments defined in [13]. Then, WAVE simulations using ns-3 [20] are carried out with the previously generated mobility scenario. Finally, The traces to emulate the mobility scenario are selected, choosing a probe vehicle and writing a .cvs file with the complete scenario information.
- Phase 2: In the real-time phase, the BSM messages of the transmitting vehicles are first created according to the J2735 standard and from the information in the .csv file. Secondly, the simulation conditions generated with ns-3 are replayed via SDR. One transmitting SDR sums the transmission of all neighbouring vehicles of the probe vehicle, implemented in the receiving SDR.

The steps and tools of each phase are further described next.

A. SUMO and 3GPP scenarios

We choose the mobility scenarios proposed by 3GPP [13], defined for Rel. 16 NR V2X but representative for DSRC, too. SUMO has been used to simulate urban and highway environments with the parameters shown in Table I.

3GPP defines three types of vehicles for system level simulations, from which we have selected type 2 (passenger vehicle with higher antenna position) with the following dimensions: 5 m length, 2 m width, 1.6 m height, and 1.6 m antenna height. More parameters are shown in Table I.

B. WAVE simulation with ns-3

The WAVE module in ns-3 involves the 802.11p PHY and MAC, the multi-channel MAC extension in 1609.4 and the 1609.3 network and transport layer. WAVE models for layers above IEEE 1609.3, namely the 1609.2 security layer and the application layer with the BSM generation, are not implemented.

Using ns-3, the vehicles are generated according to the traffic models defined in Table I. The model sets up a network of (vehicular) nodes broadcasting BSM at regular intervals plus one receiving-only vehicle. BSM obtained on the receiving vehicle will be reproduced using SDR transmitter following the same sequence as in the simulation in WAVE. Since ns-3 does not implement the application layer, dummy messages of the size corresponding to each simulated model are sent.

C. BSM message generation and encapsulation using Pycrate and V2Verifier.

The next step is to recreate, using an SDR transmitter, the scenario generated in III-B from the point of view of a receiving vehicle chosen in the simulation – the *probe* vehicle. Messages will be transmitted following the same simulation pattern. In addition, the security layer (IEEE 1609.2) and the application layer with the BSM messages coding (SAE J2735) are added only in SDR transmitter. *Pycrate* will encode the BSM messages following the J2735 standard, *V2Verifier* will encapsulate them in the application layer and apply the security layer to each frame. These layers were not implemented in the simulations using ns-3 and only dummy messages without security were used.

Pycrate [21] provides a runtime for encoding and decoding data structures for various protocols and file formats. A J2735 BSM message encoder/decoder is generated from the standard in ASN.1 format using the available compiler. Messages are encoded and decoded in real time as they can be generated with current GPS information.

V2Verifer [14] is an open-source project dedicated to wireless experimentation focused on the security of V2V communications. V2Verifier features an entirely implementation of the WAVE protocol stack together with the IEEE 1609.2 security protocol. V2Verifier uses Universal Software Radio Peripheral (USRP) to emulate vehicles exchanging Secure Protocol Data Unit (SPDU), which are BSM secured using 1609.2 protocols.

The generation time field, found in the security header of IEEE 1609.2 [22], has been used to inject the timestamp at the time the SPDU was generated using the clock provided by the GPS module. It is represented in 64 bits in units of microseconds. When the message is received, the generation time field is read and compared to the current time on the receiver. Notice that transmitter and receiver have a common time source through GPS. In this way, it is possible to reliably measure delays between both devices.

D. SDR transmitter and receiver

Two USRP B210 boards with the respective GPSDO modules have been used to perform transmission and reception with SDR devices. The GPSDO provides a high-accuracy signal to nanoseconds and provide a good reference for timing applications, which allows to build systems that serve with improved frequency accuracy (75 ppb in unlocked condition) or global timing alignment ($\pm$50 ns in locked condition). The communication between USRPs is through RF cable connection. The software used for the transmitter and receiver is the GNURadio implementation of V2Verifier with some modifications and additions for the scope of this study. First of all, it has been optimized to support high BSM message rates, particularly the 10 ms required in the most challenging 3GPP traffic model 2. Moreover, real-time encoding and decoding of BSM messages using J2735 standard has been added and the GPSDO timestamp is injected in the transmitter and compared to the GPSDO timestamp in the receiver.

TABLE I
VEHICLE DROPPING, DATA TRAFFIC MODELS & PHY/MAC PARAMETERS [13]

Vehicle Dropping		
Parameter	**Urban grid**	**Highway**
Vehicle type*	2	2
Clustered dropping	Not used	Not used
Speed	60 km/h	120 km/h
Density	5 veh/km	25 veh/km
Intersection	0.5 prob. of going straight 0.25 prob. of turning left 0.25 prob. of turning right	Not applicable
**Note: Vehicle type 2 for frequencies below 6 GHz assumes a rooftop antenna*		
Data Traffic Models		
Parameter	**Model 1**	**Model 2**
Inter-packet arrival time	100 ms	10 ms
Packet size	400 Bytes	800 Bytes
PHY/MAC parameters		
Parameter	**Model 1**	**Model 2**
Modulation	BPSK 1/2	BPSK 1/2
Rx sensitivity	-101 dBm	-101 dBm
Tx power	20 dBm	20 dBm
Antenna model	Isotropic	Isotropic
Antenna gain	0 dB	0 dB
Channel model	3GPP Urban	3GPP Highway
Frame capture margin	5 dB	5 dB

E. Delay contributors

V2X communication through the SDR implementation involves delays that need to be characterized in order to distinguish the delays inherent to the software and hardware implementation with SDR from those delays that are to be measured in the emulation of the recreated scenario.

Three sources of latency can be identifed in the system implementarion (Fig. 2):

- Application latency. This latency is associated with V2verifier and Pycrate. V2verifier provides the delay due to packet encoding/decoding at the application layer, the network and transport layer (1609.3) and the security

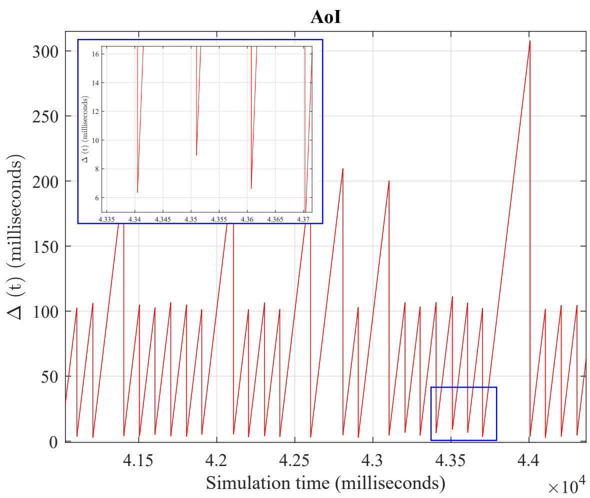

Fig. 4. AoI as measured in a realization along time.

layer (1609.2). Pycrate contributes to the delay due to the BSM message (J2735) encoding/decoding.

- GNU Radio latency due to the MAC and PHY layers (IEEE 802.11p) and the inherent buffers for signal processing [23].
- USRP and USRP hardware driver (UHD) latency.

IV. Experimental results

Before evaluating of the end-to-end timing metrics, several sanity-checks of the testbed have been carried out to ensure its validity. In the characterization of the delay contributors, it was found that the processing and protocols of the upper layers, implemented with V2Verifier and Pycrate, added 0.5 ms to the total delay, whereas the lower layers in GNU radio represented 0.8 ms and 0.5 ms in the transmitter and receiver, respectively. These values are compatible with the timing requirements of DSRC and therefore demonstrate the real-time potential of the testbed. Moreover, the experimental results have been compared to purely ns-3 simulations, i.e., replacing the 802.11p and RF transmission by the ns-3 implementation.

In the GNU and ns-3 simulations, packets are transmitted with 3 Mbps data rate, and a total bandwidth of 10 MHz bandwidth is used and centered around 5.89 GHz. All vehicles use a transmission power of 20 dBm and the time-synchronization accuracy of GPS devices is 50 ns.

Fig. 4 shows an exemplary realization of the time evolution of the age process in the highway case and traffic model 1. These are the messages received in the probe vehicle from another vehicle that is accompanying it at a distance of less than 50 meters. The AoI grows as the time since the BSM was sent is longer, until a new packet is sent after 100 ms. The mean AoI in ideal conditions – i.e., instantaneous and lossless packet reception and instantaneous BSM generation – would be 50 ms. The different delay sources increase the AoI. On the one hand, the values of the age immediately after packet reception exhibits small variations (detail in the top left corner of Fig. 4), due to the differences in the BSM generation, in the transmission delay and in the hardware delays. On the other hand, the high peaks and its variance are mainly due to MAC collisions and/or losses.

Fig. 5 and 6 show the Cumulative Density Function (CDF) of the average PAoI for the urban scenario with the traffic models in Table I and evaluated using eq. (4). For each pair transmitting vehicle - probe vehicle, the average PAoI is computed. Different colours correspond to the maximum distance between transmitting and probe vehicle considered for the computation of the metric. This maximum distance is set to 50 m, 200 m and 500 m. The dotted line corresponds to the purely ns-3 evaluations and the dot markers, labelled *SDR*, to the testbed with the hardware platform. Intervals between BSM over 10 s have been ignored, and a total of 300 s is evaluated. In all cases, the real experiments fit very closely the simulations[1].

For traffic model 1 and distances up to 50 meters, the minimum average PAoI is about 100 ms, close to the ideal 100 ms. In the considered scenario, with inter-packet arrival time of 100 ms and packet size of 400 bytes, collisions are not very likely. The main reason of the increased PAoI in distances between vehicles greater than 50 meters is the Non-line of Sight (NLOS) conditions and resulting packet loss. It is worth noticing that the generated urban grid has 250 m of distance between adjacent streets. Therefore, it is very likely that at distances up to 200 m (blue curve) and especially up to 500 m (green curve), periods of Line of Sight (LOS) and NLOS begin to intersperse. This leads to packet losses that increase the PAoI. For traffic model 2 (more frequent transmissions and longer packets), the average PAoI at the 90th percentile is more than 4 times the inter-packet period (10 ms) for distances up to 50 m. Notice, however, that conditions are more challenging and the minimum average PAoI (16 ms) has been increased by 60% compared to the inter-packet period (10 ms).

Fig. 7 and 8 show the same results as Fig. 5 and 6 but for a highway. The same line and colour coding is used. Intervals between BSM over 5 s have been ignored, and a total of 60 s and 2 km is evaluated. It is observed that the 90th percentile of the average PAoI reaches more than 500 ms in traffic model 1 and distances up to 500 m. In model 2, 90th percentile is approx. 300 ms, i.e., 30 times the inter-packet period (10 ms). Despite the fact that the number of vehicles is greater, the absence of obstacles on the highway makes it possible to obtain lower average PAoI values at greater distances. Model 2 with distances up to 50 m exhibits the worst behavior, with a 90th percentile greater than 50 ms. This is due to the fact that the most extreme conditions converge in this model: a greater number of vehicles, a high frequency of messages and a larger packet size. This configuration cause congestion to occur in the scenario and, since there is no queue in CSMA/CA for 802.11p, the messages are discarded.

There is an inherent tradeoff between age and reliability, and this is visible in our experiments when we compare the

[1]Notice that the small differences can be further adjusted if needed to better reflect in ns-3 the impact of processing delays and other non-idealities related to the use of a real hardware platform.

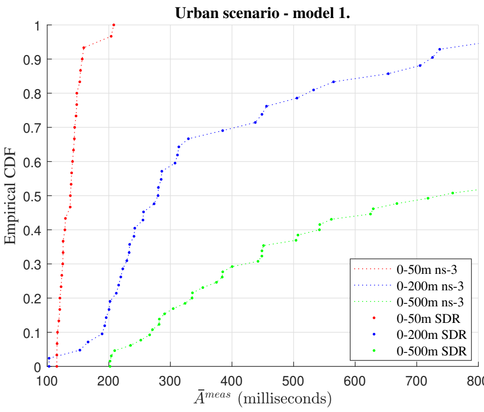

Fig. 5. CDF of the average PAoI. Urban case and traffic model 1.

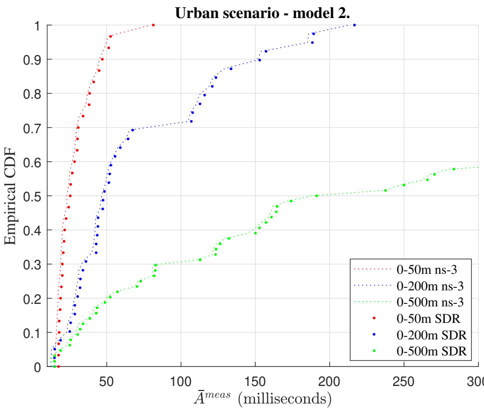

Fig. 6. CDF of the average PAoI. Urban case and traffic model 2.

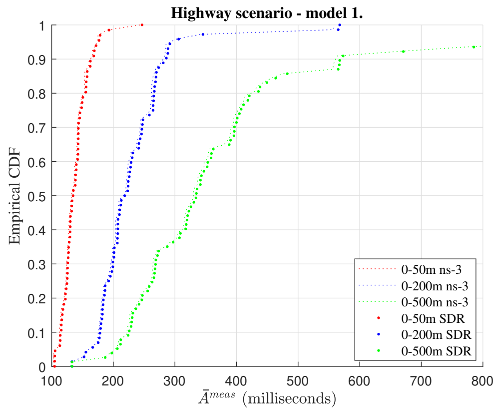

Fig. 7. CDF of the average PAoI. Highway case and traffic model 1.

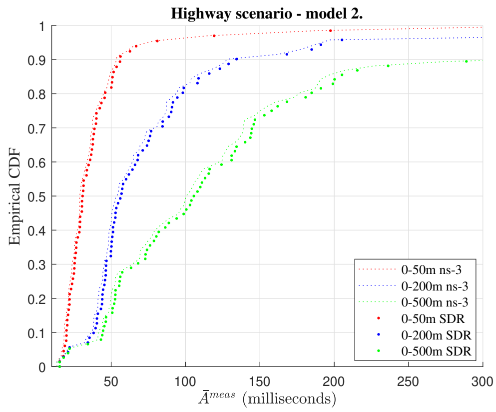

Fig. 8. CDF of the average PAoI. Highway case and traffic model 2.

previous PAoI results with the PDR plotted in Fig. 9 for the four cases. Reducing the inter-BSM period from 100 ms to 10 ms results in a significant reduction in the PDR. Moreover, the urban and highway scenarios exhibit a similar PDR for small distances, but as the distance increases, particularly for distances larger than the inter-street distance of 250 m, the propagation conditions in the urban scenario lead to a significant packet loss.

Finally, Fig. 10 and 11 depict the packet delay of the urban and highway scenarios, respectively. As in the PAoI, we compare the testbed results with a full ns-3 simulation, plotted in the left boxes. The shown delays include the channel and PHY transmission effects as well as all the processing required for the packet transmission and reception. It is observed that an inter-BSM of 10 ms can be challenging particularly for the highway scenario, where the median delay is already close to 4 ms. This is also in line with the PDR results discussed before. It is also observed that the increase in the delay in SDR with respect to the simulation in ns-3, for the case of highway, is transferred to the representation of the CDF for SDR with displacement of the dot markers to the right due to the increase in delay introduced by the hardware. Despite this small difference, our experiments show that the implemented testbed with commercial off-the-shelf components is compatible with the DSRC timing requirements.

V. Conclusions and Future Work

We have demonstrated the possibilities for implementing a DSRC testbed based on open-source software meeting the timing requirements of the 802.11p lower layers using low-cost, commercial off-the-shelf components. The real-time testbed is supported by a scenario generation phase based on ns-3 and using 3GPP reference models. Moreover, our implementation includes those layers not included in ns-3, namely the 1609.2 security layer and the BSM encoding, resulting in a full-stack testbed. The testbed has been used to characterize the different contributors to the total delay budget, the AoI and the PDR. Time stamping and AoI measurements have been done on the real device via GPSDO, as in a real scenario. Our results show that more frequent BSM transmission reduces the average PAoI but with a higher value relative to the inter-BSM period, owing to the unavoidable tradeoff between age and reliability. The future work includes updates in the sofware and hardware to be fully compliant with the specifications of SAE J2945/1 in terms of modulation (QPSK) and congestion control. Another avenue of future work aims at optimizing the communication parameters to minimize the average PAoI and mapping the age to relevant application metrics that evaluate, e.g., the risk of collision.

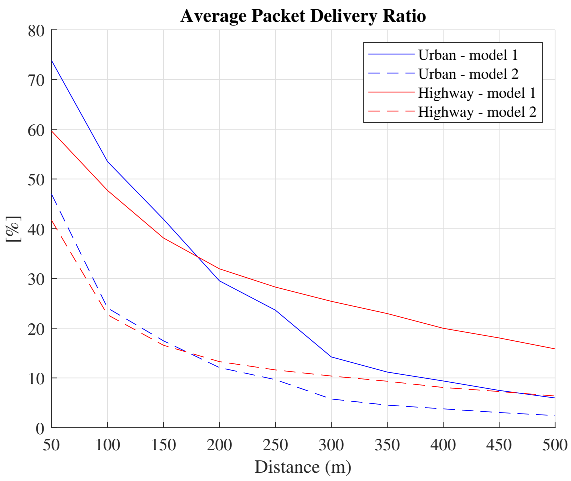

Fig. 9. Average PDR for the receiver vehicle during the simulated period.

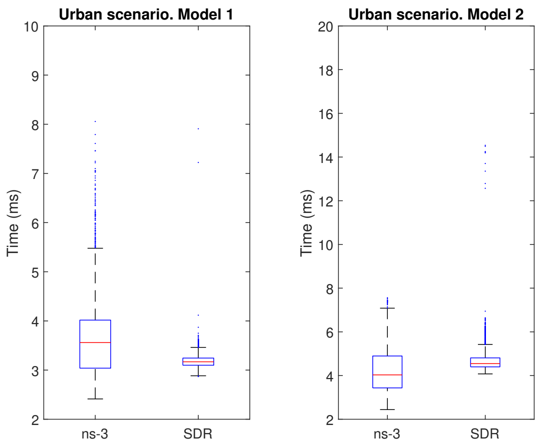

Fig. 10. Delay. Urban scenario. Comparison between the simulation in ns-3 and the realization with SDR.

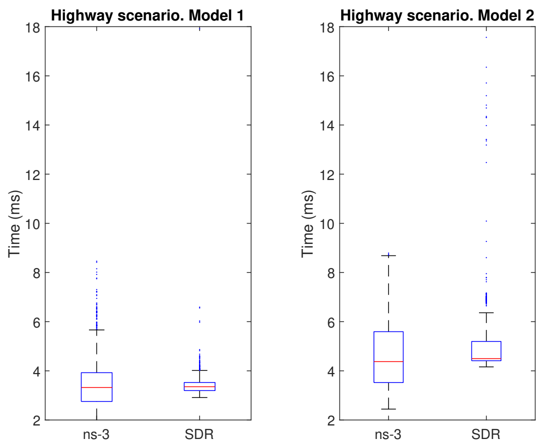

Fig. 11. Delay. Highway scenario. Comparison between the simulation in ns-3 and the realization with SDR.

ACKNOWLEDGMENT

This work was funded in part by Junta de Andalucía, the European Union and the European Fund for Regional Development FEDER through grants P18-RT-3175, P18-TP-3587 and UMA20-FEDERJA-002.

REFERENCES

[1] J. B. Kenney, "Dedicated short-range communications (dsrc) standards in the united states," *Proc. of the IEEE*, vol. 99, no. 7, 2011.
[2] S. Kaul, R. Yates, and M. Gruteser, "Real-time status: How often should one update?" in *International Conference on Computer Communications (INFOCOM)*, Mar. 2012, pp. 2731–2735.
[3] M. A. Abd-Elmagid, N. Pappas, and H. S. Dhillon, "On the role of age of information in the Internet of Things," *IEEE Communications Magazine*, vol. 57, no. 12, pp. 72–77, Dec. 2019.
[4] R. D. Yates and et al, "Age of information: An introduction and survey," *IEEE Jour. on Selected Areas in Comms.*, vol. 39, no. 5, 2021.
[5] H. B. Beytur, S. Baghaee, and E. Uysal, "Measuring age of information on real-life connections," in *27th Signal Processing and Communications Applications Conference (SIU)*, Apr. 2019.
[6] L. Cao, H. Yin, J. Hu, and L. Zhang, "Performance analysis and improvement on DSRC application for V2V communication," *ArXiV Preprint arXiv:2102.07023*, Feb. 2021.
[7] P. Popovski, F. Chiariotti, K. Huang, A. E. Kalør, M. Kountouris, N. Pappas, and B. Soret, "A perspective on time toward wireless 6g," *Proceedings of the IEEE*, vol. 110, no. 8, pp. 1116–1146, 2022.
[8] B. Choudhury, V. K. Shah, A. Dayal, and J. H. Reed, "Joint age of information and self risk assessment for safer 802.11p based v2v networks," *ArXiV Preprint arXiv:2012.04774*, Dec. 2020.
[9] A. Baiocchi and I. Turcanu, "Age of information of one-hop broadcast communications in a csma network," *IEEE Communications Letters*, vol. 25, no. 1, pp. 294–298, 2021.
[10] J.-K. Bae, M.-C. Park, E.-J. Yang, and D.-W. Seo, "Implementation and performance evaluation for dsrc-based vehicular communication system," *IEEE Access*, vol. 9, pp. 6878–6887, 2021.
[11] B. Bloessl, M. Segata, C. Sommer, and F. Dressler, "Towards an open source ieee 802.11p stack: A full sdr-based transceiver in gnu radio," in *2013 IEEE Vehicular Networking Conference*, 2013, pp. 143–149.
[12] M. Klapež, C. A. Grazia, and M. Casoni, "Experimental evaluation of ieee 802.11p in high-speed trials for safety-related applications," *IEEE Transactions on Vehicular Technology*, vol. 70, no. 11, 2021.
[13] 3GPP, "Study on evaluation methodology of new vehicle-to-everything (V2X) use cases for LTE and NR," 3GPP, Technical Recommendation (TR) 37.885, June 2019, version 15.3.0.
[14] G. Twardokus, J. Ponicki, S. Baker, P. Carenzo, H. Rahbari, and S. Mishra, "Targeted discreditation attack against trust management in connected vehicles," in *Proc. IEEE Int. Conf. Communications (ICC)*, Montreal, Canada, Jun. 2021.
[15] DLR. "SUMO documentation". [Online]. Available: https://sumo.dlr.de/docs/index.html
[16] SAE, "Dedicated Short Range Communications (DSRC) Message Set Dictionary," Soc. Autom. Eng. (SAE) International, Tech. Rep. J2735, Jul 2020, version j2735_202007.
[17] K. F. Hasan, Y. Feng, and Y.-C. Tian, "GNSS time synchronization in vehicular Ad-Hoc networks: Benefits and feasibility," *IEEE Transactions on Intelligent Transportation Systems*, vol. 19, no. 12, 2018.
[18] IEEE, "IEEE standard for information technology– local and metropolitan area networks– specific requirements– part 11: Wireless LAN medium access control (MAC) and physical layer (PHY) specifications amendment 6: Wireless access in vehicular environments," 2010.
[19] B. Barakat, H. Yassine, S. Keates, I. Wassell, and K. Arshad, "How to measure the average and peak age of information in real networks?" in *European Wireless 2019; 25th European Wireless Conference*, 2019.
[20] ns-3. ns-3 — a discrete-event network simulator for internet systems. [Online]. Available: https://www.nsnam.org/
[21] P. Security, "Pycrate," https://github.com/P1sec/pycrate, 2022.
[22] "IEEE standard for wireless access in vehicular environments–security services for applications and management messages," *IEEE Std 1609.2-2016 (Revision of IEEE Std 1609.2-2013)*, pp. 1–240, 2016.
[23] N. B. Truong, Y.-J. Suh, and C. Yu, "Latency analysis in gnu radio/usrp-based software radio platforms," in *MILCOM 2013 - 2013 IEEE Military Communications Conference*, 2013, pp. 305–310.